Supporting Information

The Impact of Carbon Support Functionalization on the Electrochemical Stability of Pt Fuel Cell Catalysts

*Henrike Schmies[1], Elisabeth Hornberger[1], Björn Anke[2], Tilman Jurzinsky[3], Hong Nhan Nong[1,5], Fabio Dionigi[1], Stefanie Kühl[1], Jakub Drnec[4], Martin Lerch[2], Carsten Cremers[3], Peter Strasser[1]**

[1] Department of Chemistry, Chemical Engineering Division, Technical University of Berlin, Berlin, Germany

[2] Institute of Inorganic Chemistry, Technical University Berlin, Berlin, Germany

[3] Fraunhofer-Institut für Chemische Technologie ICT, Pfinztal, Germany

[4] European Synchrotron Radiation Facility (ESRF), Grenoble, France

[5] Max Planck Institute for Chemical Energy Conversion, Stiftstr. 34-36, 45470 Mülheim an der Ruhr, Germany

*Email: pstrasser@tu-berlin.de

Table S1. Elemental bulk and surface composition in at% of unmodified Vulcan, O-Vulcan and N-Vulcan 400°C and 800°C from elemental analysis, hot gas extraction and XPS.

[at%]	**N** bulk from elemental analysis	**C** bulk from elemental analysis	**H** bulk from elemental analysis	**N** bulk from hot gas extraction	**O** bulk from hot gas extraction	**N** surface from XPS	**O** surface from XPS	**C** surface from XPS	**Ti** (substrate) surface from XPS
Vulcan	0.00	98.10	0.00	-	-	0	5.84	92.16	2.00
O-Vulcan	0.19	85.58	0.38	0.268	12.6	0.73	12.61	86.15	0.51
N-Vulcan 400°C	2.53	93.26	0.13	2.5	2.9	3.86	9.35	83.35	3.44
N-Vulcan 800°C	1.53	95.08	0.02	1.8	0.85	2.26	7.3	87.38	3.07

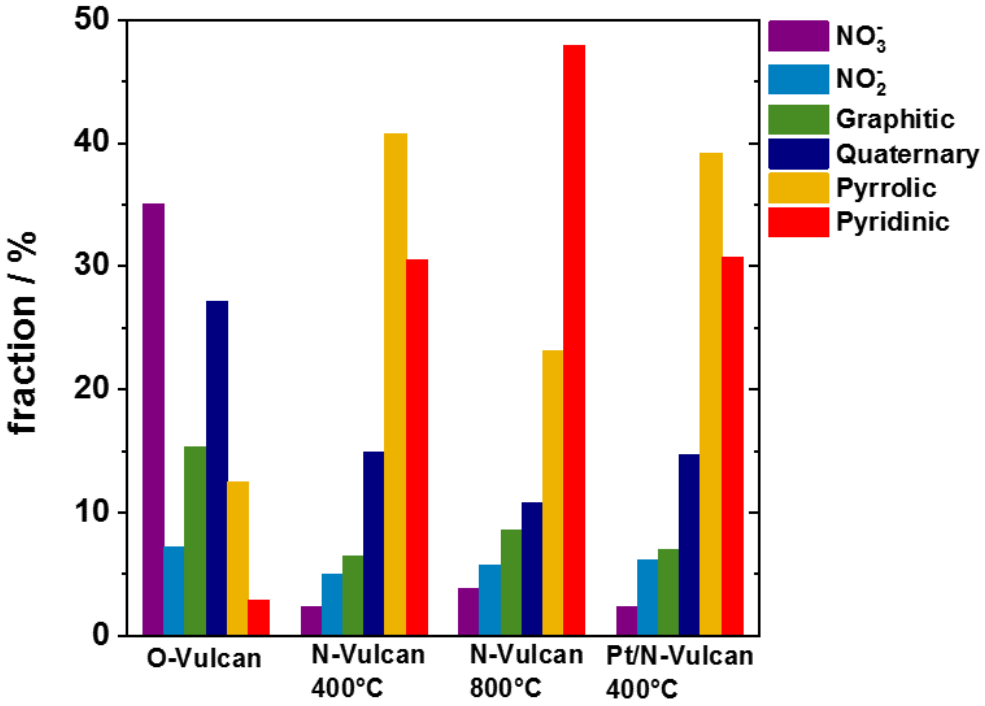

Figure S1. Fractions of the different N-moieties from deconvolution of the N 1s spectra in the modified carbons and in Pt/N-Vulcan 400°C.

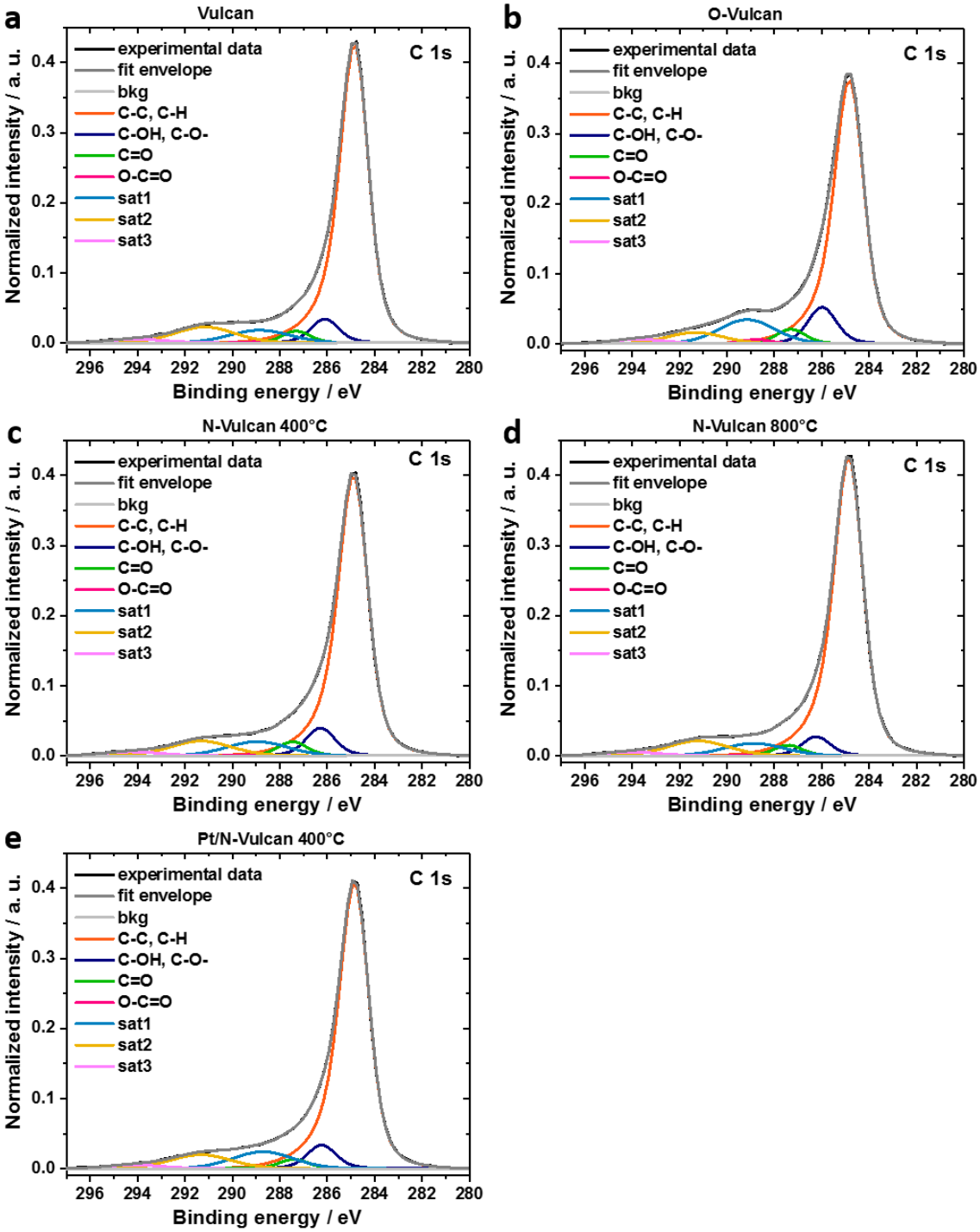

Figure S2. XPS C 1s spectra and individual peak deconvolution for unmodified Vulcan (a), O-Vulcan (b), N-Vulcan 400° (c), N-Vulcan 800°C (d) and for Pt/N-Vulcan 400°C (e).

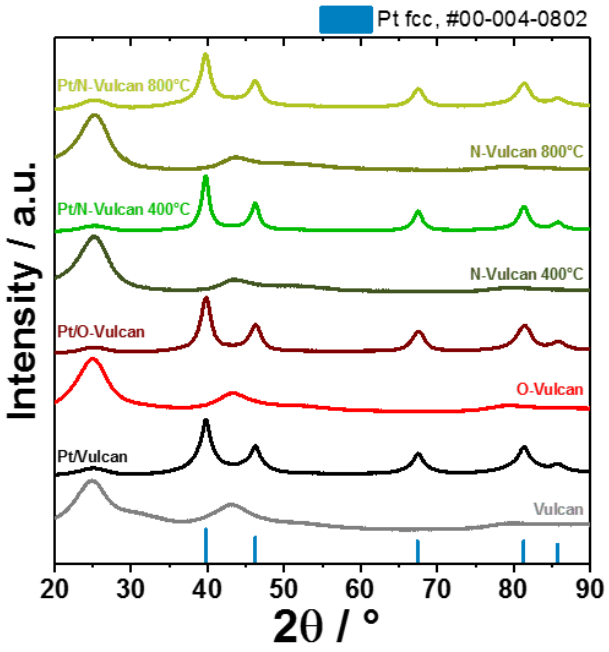

Figure S3. X-ray powder diffraction patterns of the modified and unmodified carbon supports and the respective Pt electrocatalysts. Vertical blue lines represent the reference pattern for fcc Pt (PDF#00-004-0802).

Table S2. Pt weight loading (wt%) from ICP-OES.

	wt%
Pt/Vulcan	20.1
Pt/O-Vulcan	23.1
Pt/N-Vulcan 400°C	19.8
Pt/N-Vulcan 800°C	20.9

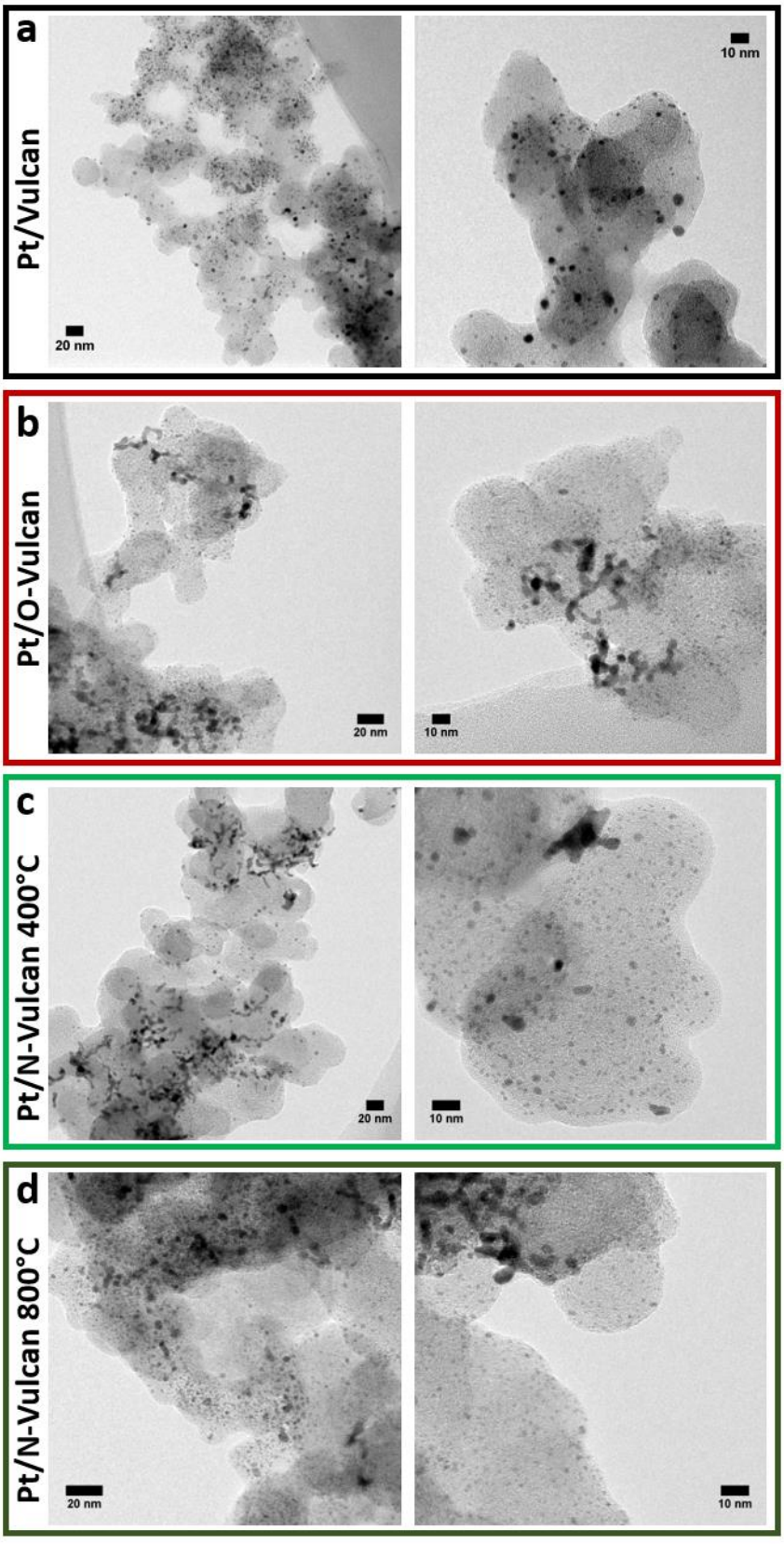

Figure S4. TEM images for Pt on unmodified Vulcan (a), O-Vulcan (b), N-Vulcan 400°C (c), and N-Vulcan 800°C (d).

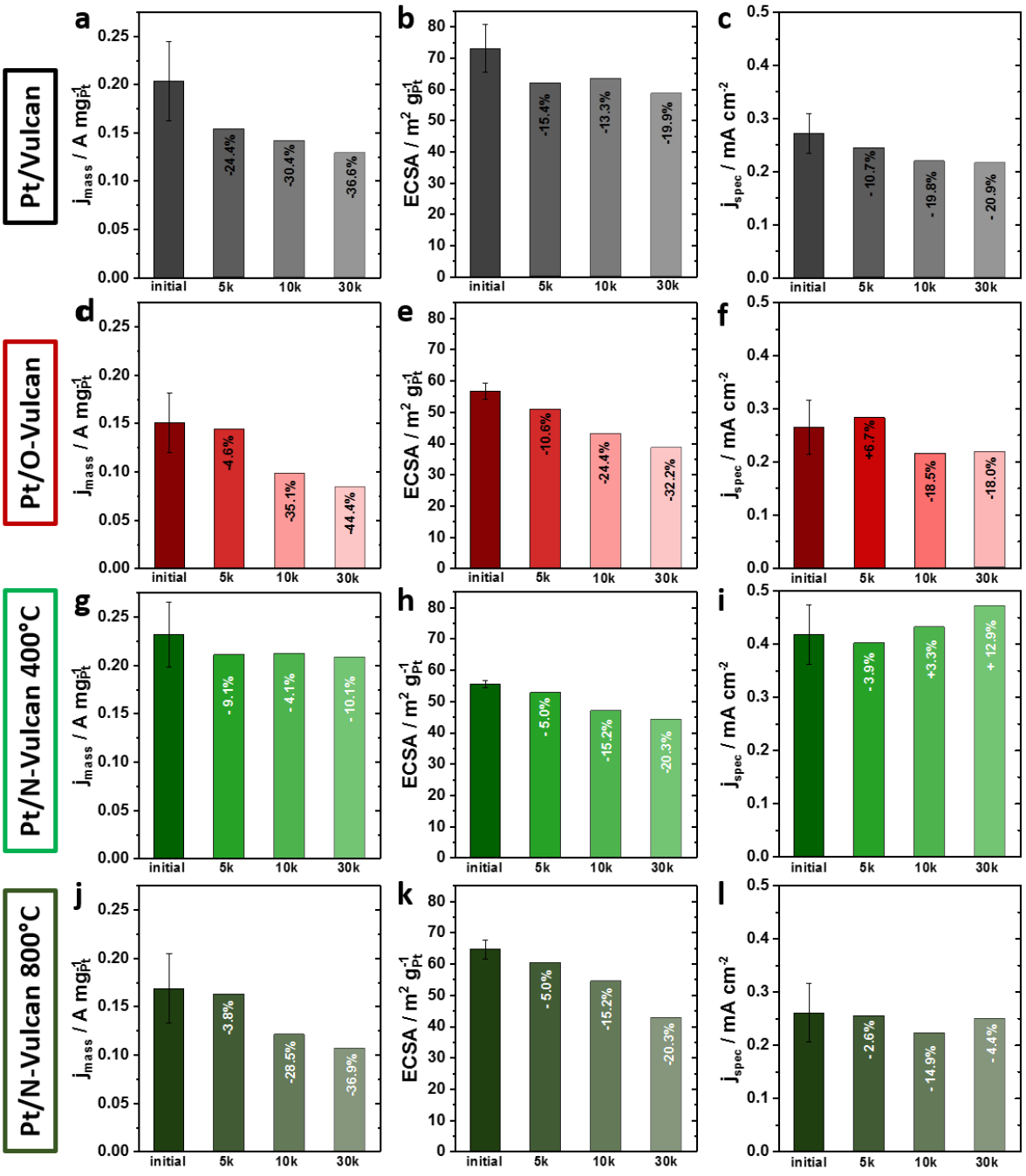

Figure S5. Results from AST for 5k, 10k and 30k cycles from 0.6-0.95 V in Nitrogen-saturated 0.1 M $HClO_4$ for Pt/Vulcan, Pt/O-Vulcan, Pt/N-Vulcan 400°C and Pt/N-Vulcan 800°C as a function of mass activity at 0.9 V j_{mass}(a,d,g,j), ECSA (b,e,h,k) and specific activity j_{spec} (c,f,i,l).

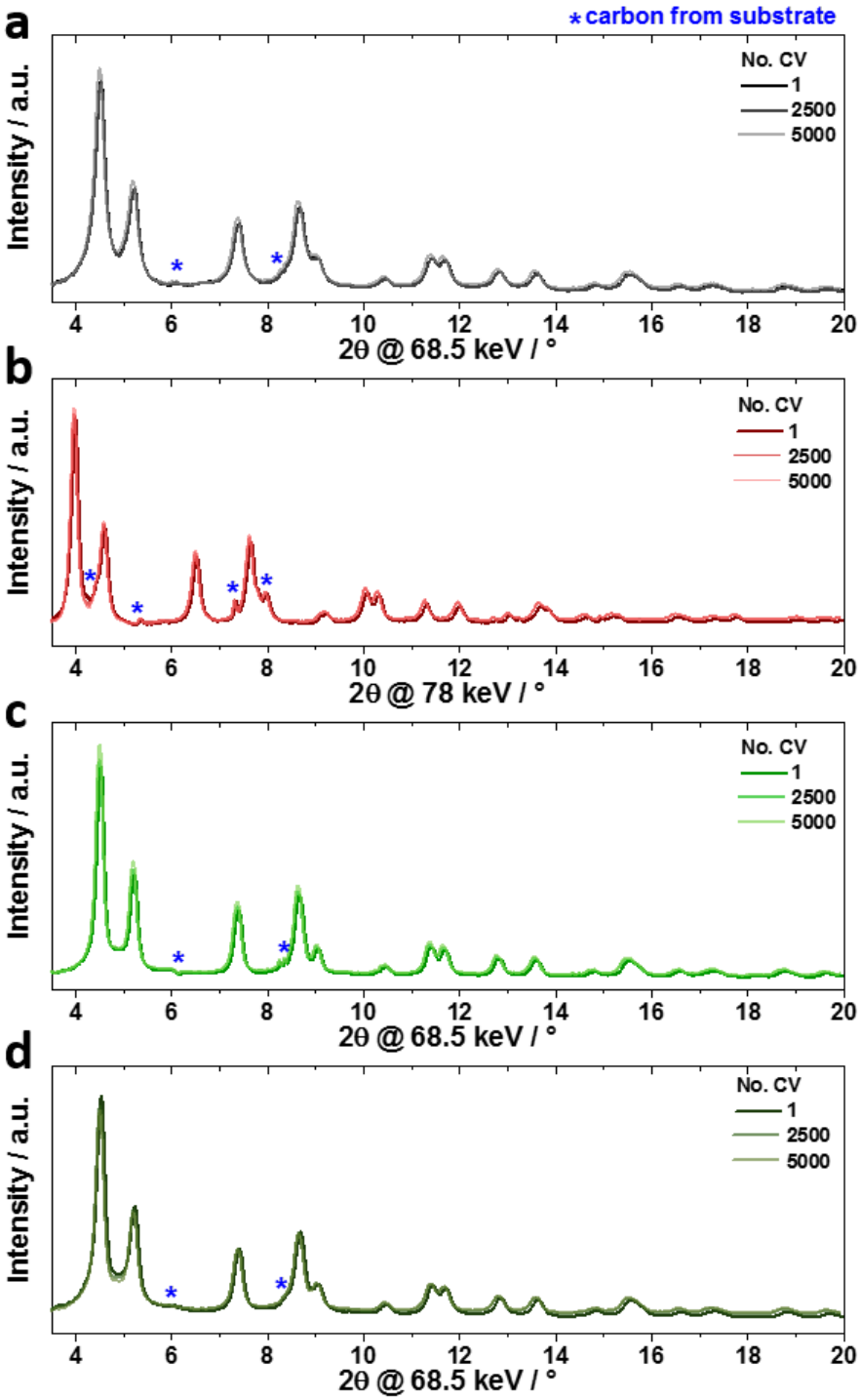

Figure S6. *In situ* high energy X-ray diffraction patterns over 5k cycle of the AST for Pt/Vulcan (a), Pt/O-Vulcan (b), Pt/N-Vulcan 400°C (c) and Pt/N-Vulcan 800°C (d).

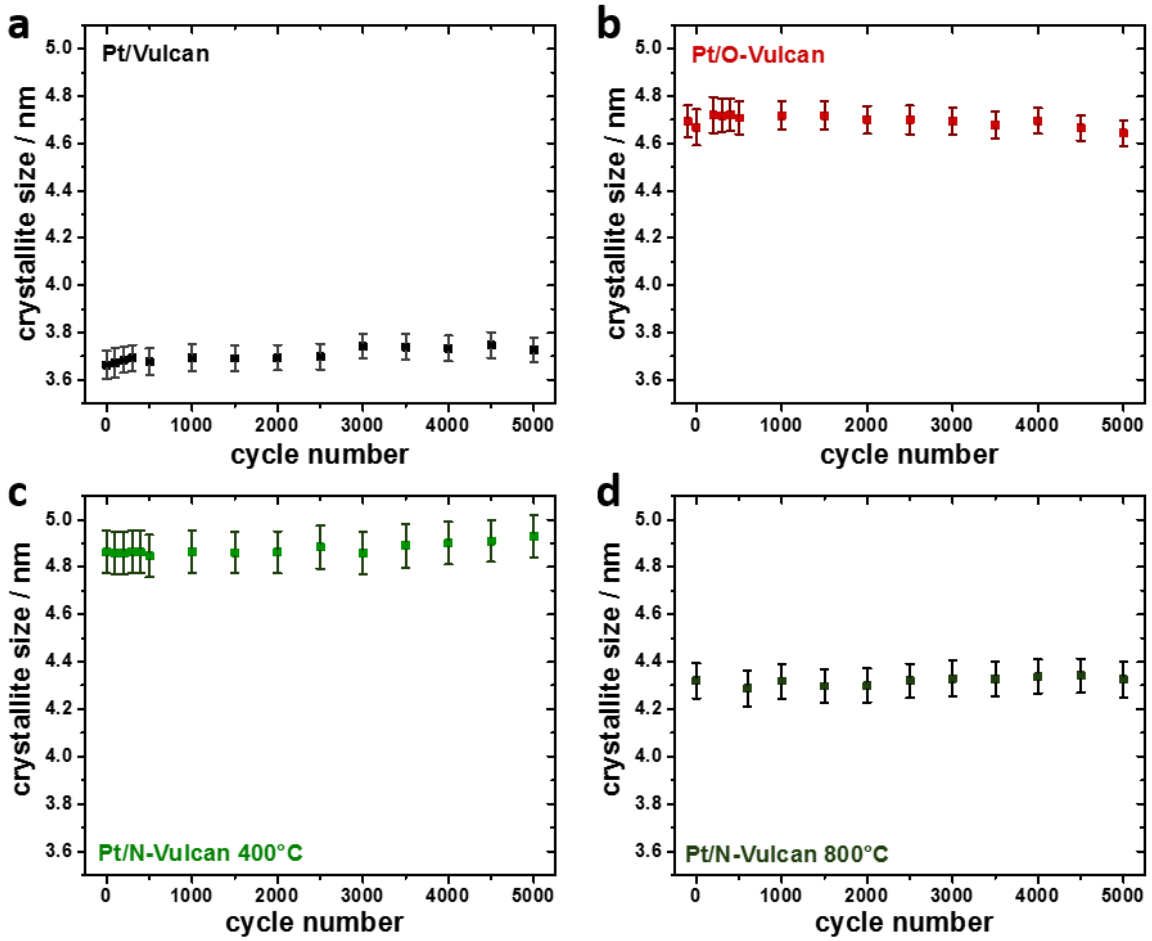

Figure S7. Crystallite size from Rietveld refinement of the *in situ* high energy X-ray diffraction patterns over 5k cycle of the AST for Pt/Vulcan (a), Pt/O-Vulcan (b), Pt/N-Vulcan 400°C (c) and Pt/N-Vulcan 800°C (d).

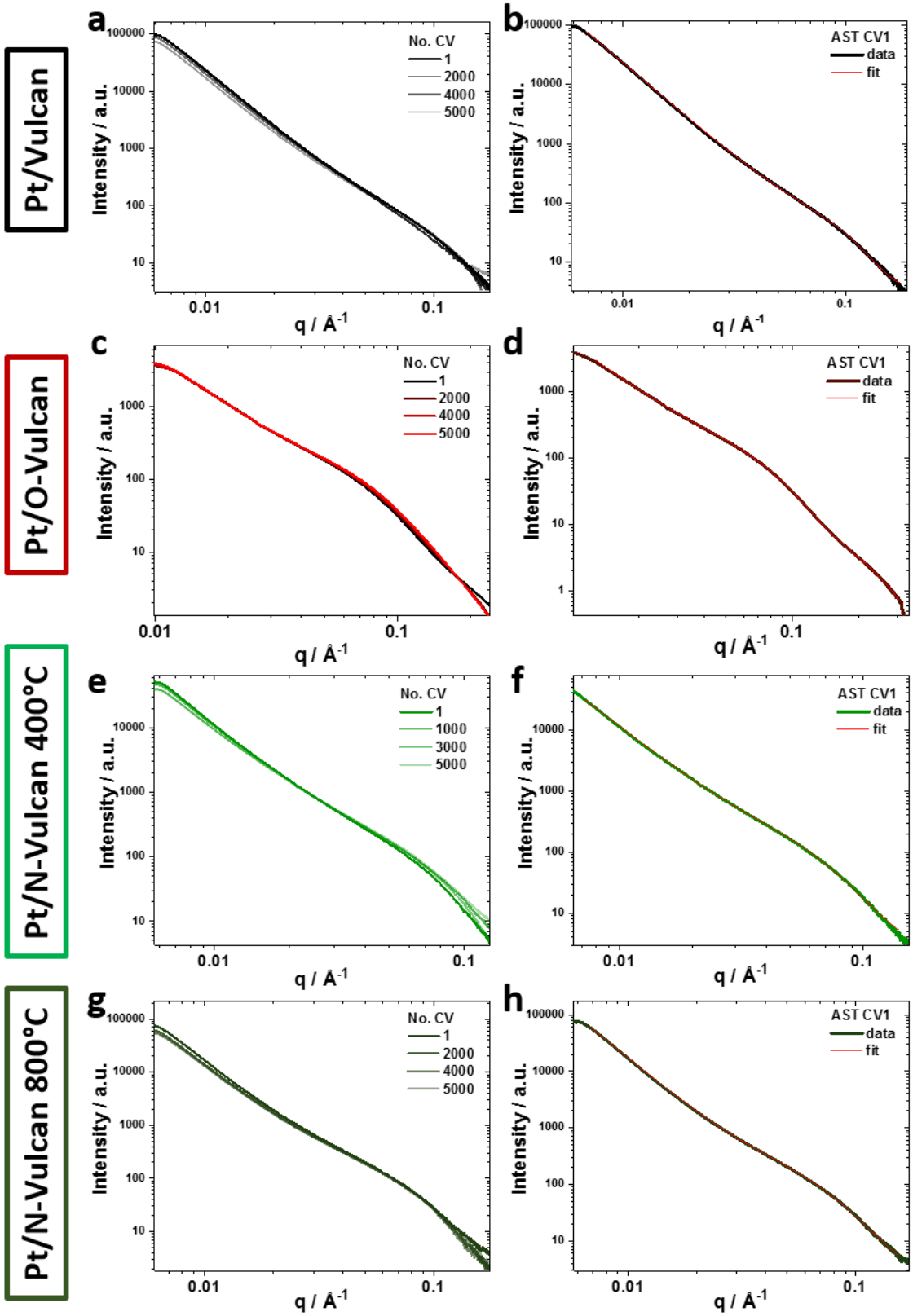

Figure S8. *In situ* small angle X-ray scattering curves over 5k cycle of the AST for Pt/Vulcan, Pt/O-Vulcan, Pt/N-Vulcan 400°C and Pt/N-Vulcan 800°C (a,c,e,g) and scattering curves at start of the AST including the individual fit curves (b,d,f,h).

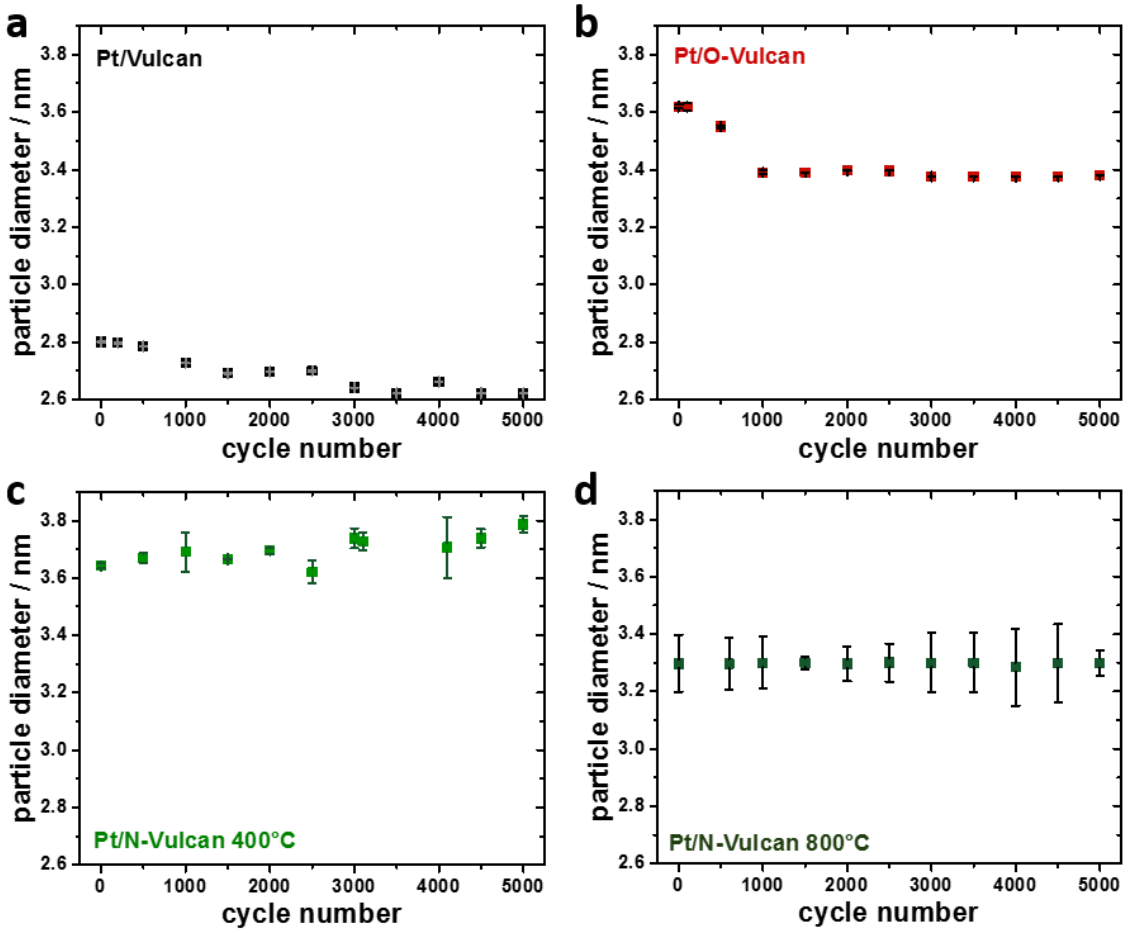

Figure S9. Mean particle diameter from fit of the *in situ* small angle X-ray scattering curves over 5k cycle of the AST for Pt/Vulcan (a), Pt/O-Vulcan (b), Pt/N-Vulcan 400°C (c) and Pt/N-Vulcan 800°C (d).